

# Characterization of the $\text{In}_{0.53}\text{Ga}_{0.47}\text{As } n^+nn^+$ Photodetectors

Fatima Zohra Mahi, Luca Varani

**Abstract**—We present an analytical model for the calculation of the sensitivity, the spectral current noise and the detective parameter for an optically illuminated  $\text{In}_{0.53}\text{Ga}_{0.47}\text{As } n^+nn^+$  diode. The photocurrent due to the excess carrier is obtained by solving the continuity equation. Moreover, the current noise level is evaluated at room temperature and under a constant voltage applied between the diode terminals. The analytical calculation of the current noise in the  $n^+nn^+$  structure is developed by considering the free carriers fluctuations. The responsivity and the detection parameter are discussed as functions of the doping concentrations and the emitter layer thickness in one-dimensional homogeneous  $n^+nn^+$  structure.

**Keywords**—Responsivity, detection parameter, photo-detectors, continuity equation, current noise.

## I. INTRODUCTION

ONE of the most critical parts in fiber communication system is the receiver of the optical signal. Optical receiver in a digital communication system contains the photodetectors, transimpedance amplifier, and post amplifier then followed by decision circuit. In particular, the photodetector (PD) produces photocurrent proportional to the incident optical power. As a consequence, the appropriate choice of the photodetector depends on the photocurrent value which is proportional to the efficiency absorption of photons, the concentration of the emitter layer and the optical incident power.

The performance of the photo-detectors for optical systems applications has improved as a result of the improvements in materials and the development of the advanced device structures. The homojunction structures have been demonstrated as wavelength tunable infrared detectors in recent years. This concept was successfully tested on Si [1], Ge and  $\text{In}_x\text{Ga}_{1-x}\text{As}$  materials [2]. In particular, the unipolar nanodiode (as  $n^+nn^+$  structure) has shown experimentally a good responsivity and noise properties for microwave and terahertz detection [3].

Therefore, due to the high absorption coefficient, the In-GaAs absorption region is typically a few micrometers thick and can achieve the wavelength range from 0.1  $\mu\text{m}$  to 2  $\mu\text{m}$ .

Moreover, the essential optical parameter that characterizes the photodetector is the photosensitivity to light. It is defined

as the ratio of the photocurrent to the incident light power at a given wavelength.

The random fluctuations in a detector's output limit its responsivity to a certain minimum detectable power. The power necessary to generate an output signal equal to the noise is known as the Noise Equivalent Power (NEP).

The NEP is the optical power that generates sufficient photocurrent to equal the noise current. However, the current noise level, of the structures and the materials used for the detection, determines the radiative noise arriving at the detector from the background environment [4]. In addition, the detection parameter (D), gives a meaningful comparison between different detectors, it is widely used for the infrared photodetector characterization.

This contribution presents an analytical model for the calculation of the responsivity and the detection parameter of the  $\text{In}_{0.53}\text{Ga}_{0.47}\text{As } n^+nn^+$  diode by using the current spectral density [5]. The current noise is evaluated at room temperature and under a constant voltage applied between the diode terminals. The noise calculation considers the synchronous motion of the free carriers in each region of the structure [6].

In addition, the model can calculate in a first step the sensitivity of the  $n^+nn^+$  structure to light. The analytical approach takes into account the responsivity evaluation in the wavelength range of the  $\text{In}_{0.53}\text{Ga}_{0.47}\text{As}$  absorption. In particular, the excess carriers are solved using the continuity equation for holes. Then in the second step, the detection parameter is obtained by using the spectral current noise and the sensitivity of the diode. The results are investigated at different doping concentrations and at different thickness of the emitter layer in one-dimensional inhomogeneous  $n^+nn^+$  structure.

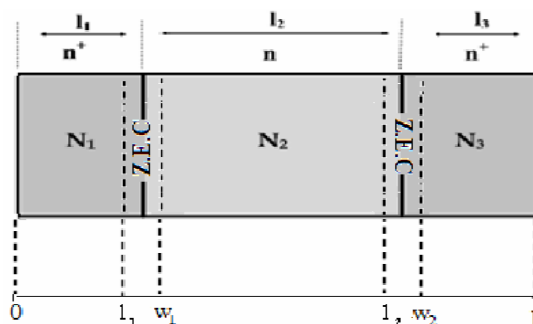


Fig. 1 Schematic view of the  $n^+nn^+$  diode with:  $l_1$  and  $l_3$  the lengths of the  $n^+$  regions,  $l_2$  the length of the  $n$  region,  $N_1 = N_3$  and  $N_2$  the doping concentrations of the three regions.

Fatima Zohra Mahi is with the Science and Technology Institute of Bechar University, Algeria, CO 80305 USA (corresponding author; e-mail: fati\_zo\_mahi2002@yahoo.fr).

Luca Varani was with the Montpellier University, France, UMR 5214. He is now with the Institute of South Electronic (e-mail: fati\_zo\_mahi2002@yahoo.fr).

## II. ANALYTICAL MODEL

The schematic structure of an  $\text{In}_{0.53}\text{Ga}_{0.47}\text{As}$   $n^+nn^+$  diode is shown in Fig. 1. Here  $l_i$  is the length and  $N_i$  is the doping of  $i$ -region. We consider a symmetrical structure with  $N_j=N_3$ ,  $l_j=l_3$  and we assume that the doping is equal to the free carrier concentration in each region of the diode.

### A. The Sensitivity

The device is illuminated along the length direction (one-dimensional  $x$ ). The photocurrent is developed across the double homojunction  $n^+n$  and  $nn^+$  due to incident light. The incident optical flux is absorbed in the  $n^+nn^+$  diode and leads to create electron-hole pairs in the depletion regions. With the choice of the device dimensions and the material, we can obtain a high sensitivity and can perform the high frequency operation of the photodetector. Here the material chosen for photodetector is the  $\text{In}_{0.53}\text{Ga}_{0.47}\text{As}$  with high mobility and high absorption coefficient at higher wavelengths, which get better responsivity [7].

In the first step, we interest to calculate the excess carrier generated in the  $n^+$  and  $n$  regions by solving the continuity equation for holes. The number of the photo-generated holes by respecting doping profiles is [7]:

$$\frac{\partial p(x,t)}{\partial t} = \frac{1}{q} \frac{\partial J_p(x,t)}{\partial x} + G - \frac{\Delta p(x,t)}{\tau_p} \quad (1)$$

where the lifetime for holes is  $\tau_p$ ,  $G$  is the volume generation rate and  $J_p$  is the holes current density given by:

$$J_p = -qD_p \frac{\partial \Delta p}{\partial x} \quad (2)$$

By using the generation rate at stationary condition, the continuity equation can be written as:

$$D_p \frac{\partial^2 \Delta p}{\partial x^2} + \frac{\Delta p}{\tau_p} - \alpha \Phi(\lambda)(1-R)e^{-\alpha x} = 0 \quad (3)$$

where  $\alpha$  is the absorption coefficient,  $D_p$  is the hole diffusion coefficient,  $\Phi(\lambda)$  is incident optical flux,  $\lambda$  is the incident wavelength and  $R$  is the reflective coefficient.

The resolution of (3) in the depletion regions and in the double homojunction  $n^+nn^+$  structure depends on the boundary conditions at the limit of each region. This leads to evaluate the current densities  $J_1, J_2, J_3, J_{d_1}$  and  $J_{d_2}$  of all photodetector.

For the first region  $n^+$ , (3) is solved by using the boundary condition at  $x = 0$  the holes excess carrier are related to the surface recombination velocity ( $S_p$ ):  $D_p \frac{\partial \Delta p}{\partial x} = S_p \Delta p$  and the condition at  $x = l_1$  is  $\Delta p = 0$ . The boundary condition for the  $n$  region at the limit  $x = l_1 + W_1$  is proportional to holes excess carriers  $\Delta p = 0$ . At the limit  $x = l_2$  the condition is given by  $\Delta p = 0$ .

Moreover, the holes excess concentration at the limit of the second region  $n^+$  of structure (at  $x = W_2$  and at  $x = L$ ) presents a continued value. The photocurrent in the depletion regions is evaluated as:

$$\begin{aligned} J_{d_1} &= q\Phi(1-R)(e^{-\alpha l_1} - e^{-\alpha W_1}) \\ J_{d_2} &= q\Phi(1-R)(e^{-\alpha l_2} - e^{-\alpha W_2}) \end{aligned} \quad \text{For } \begin{cases} l_1 \leq x \leq l_1 + W_1 \\ l_2 \leq x \leq l_2 + W_2 \end{cases} \quad (4)$$

The total current density of the depletion regions is equal to  $J_d = J_{d_1} + J_{d_2}$ . For the  $n^+nn^+$  photodetector the total current density is calculated as  $J_{ph} = J_1 + J_2 + J_3 + J_{d_1} + J_{d_2}$ . Then we can calculate the photosensitivity which is defined as the ratio of the photocurrent to the incident light power at a given wavelength:

$$S = \frac{J_{ph}}{q\Phi(1-R)h\nu} \quad (5)$$

where the incident light energy is  $h\nu$  and  $S$  is the photosensitivity of the photodetector. Equation (5) presents the dependence of the photosensitivity to the photocurrent which describes the structure parameters effect to the high sensitivity evaluation.

### B. High Frequency Spectral Current Noise

In the high frequency region, the current fluctuations in the  $n^+nn^+$  structure are described by the dynamics of the free carrier fluctuations. The structure and the analytical approach are similar to that studied in [8] when the spectra current noise is determined under a constant voltage drop at the terminals of the diode ( $\delta U = 0$ ). By using the analytical model described in [8] the spectral density in the  $n^+nn^+$  structure can be represented:

$$S_{JJ}(\omega) = \left( \omega \frac{eA}{L} \right)^2 \sum_{j=1}^3 \left| \sum_{i=1}^3 N_i l_i b_{i,j} \right|^2 S_{ff}^j \quad (6)$$

where  $S_{ff}^j = 4kT \frac{1}{A_m N_i l_i} \frac{v_i}{L}$  is the spectral density of the thermal Langevin force normalized to the free carrier number in  $i$ -region ( $k$  is the Boltzmann constant and  $T$  the lattice temperature),  $L = l_1 + l_2 + l_3$  is the total length of the diode,  $A$  is the diode cross-section, the  $b_{i,j}$  coefficients are the elements of the inverse matrix expressed by the elements:  $a_{11} = -\omega^2 + i\omega v_1 + \omega_1^2(1 - r_1)$ ,  $a_{32} = a_{12} = r_2 \omega_2^2$ ,  $a_{22} = -\omega^2 + i\omega v_2 + \omega_2^2(1 - r_2)$ ,  $a_{31} = a_{21} = r_1 \omega_1^2$ ,  $a_{23} = a_{13} = r_3 \omega_3^2$ ,  $a_{33} = -\omega^2 + i\omega v_3 + \omega_3^2(1 - r_3)$ . Here  $r_i = \frac{l_i}{L}$  are the relative lengths and  $\omega_i = \sqrt{N_i e^2 / \epsilon \epsilon_0 m}$  is the plasma frequency of  $i$ -regions.

The model of (6) is expected to describe correctly the current fluctuations in the terahertz (THz) domain. In addition, the spectrum of current fluctuations  $S_{JJ}$  in (6) can also be used, on one hand, to describe the frequency dependent noise through the term  $\omega \frac{eA}{L}$  and, on the other hand, it allows us to determine the contribution of the  $n^+$  and  $n$  regions when the dependence with position is included in  $l_i$ .

### C. Low Frequency Current Noise

In this theoretical model the possible noise contributions in low frequency ( $f < 1$  THz) such as the generation-recombination or  $1/f$  noise are not taken into account [9]. Moreover, we consider the applied voltage is sufficiently low to assume that the diode exhibits ohmic characteristics, and

then the dominant contribution to the total noise in the low frequency region comes from the thermal noise.

The thermal current noise spectrum takes the Lorentzian form given by [9]:

$$S_{low}(\omega) = \frac{4kT}{1+(\omega\tau)^2} \sum_{i=1}^3 \frac{1}{R_i} \quad (7)$$

where  $R_i$  is the resistance of  $i$ -regions and  $\tau$  is the average collision (relaxation) time defined as  $\tau = \frac{\mu_n m}{e}$  (where  $\mu_n$  is the electron mobility). The resistance of  $i$ -regions can be written as:

$$R_i = \rho_i \frac{l_i}{A_i} \quad (8)$$

where the electrical resistivity is  $\rho_i$  and  $A_i$  is the cross section of  $i$ -region. The electrical resistivity is given by:

$$\rho_i = \frac{1}{eN_i\mu_n} \quad (9)$$

The total spectrum of current fluctuations at low and high frequency is obtained by using (7) and (6):

$$S_b = S_{JJ}(\omega) + S_{low}(\omega) \quad (10)$$

Equation (10) represents the basis of our analysis of the noise spectrum of the  $n^+nn^+$  diode, which will be used for detection parameter calculation.

### III. DETECTION PARAMETER

This factor can determine the ability of the device to detect the variations of the input optical signal. The detectivity of  $n^+nn^+$  diode is determined by the rate of change of the surface charge density by using (11):

$$D = \frac{s\sqrt{A}}{\sqrt{S_b(\omega)}} \quad (11)$$

Equation (11) is obtained by using the responsivity of (5) and the spectral current noise of (10).

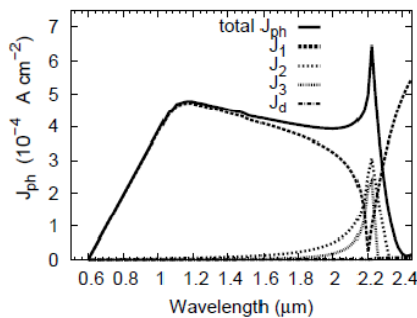


Fig. 2 Photocurrent in an  $\text{In}_{0.53}\text{Ga}_{0.47}\text{As}$   $n^+nn^+$  diode with:  $\epsilon_r = 13.8$ ,  $\mu_p = 400 \text{ cm}^2\text{Vs}^{-1}$ ,  $m^* = 0.046$ ,  $D_p = 7.5$ ,  $n_i = 9.4 \times 10^{11} \text{ cm}^{-3}$ , surface recombination velocity  $S_p = 10^4 \text{ cm.s}^{-1}$ ,  $l_1 = l_3 = 0.5 \text{ }\mu\text{m}$ ,  $l_2 = 0.25 \text{ }\mu\text{m}$ ,  $N_{1,3} = 10^{17} \text{ cm}^{-3}$  and  $N_2 = 10^{14} \text{ cm}^{-3}$ .

### IV. RESULTS AND DISCUSSION

The calculations of photocurrent have been carried out for  $\text{In}_{0.53}\text{Ga}_{0.47}\text{As}$   $n^+nn^+$  diode by considering (2) and (4). The diode is characterized by a high free carrier concentration of  $n^+$  regions  $10^{17} \text{ cm}^{-3}$ , a low concentration of  $n$  region  $10^{14} \text{ cm}^{-3}$  and a total length  $L = 1.5 \text{ }\mu\text{m}$ . Fig. 2 reports the separate photocurrent contributions coming from  $n^+$ ,  $n$  regions and the depletion regions obtained from the analytical model.

In Fig. 2, we remark that the photocurrent ( $J_{ph}$ ) results of the incident light covers the all wavelengths from  $0.6 \text{ }\mu\text{m}$  to  $2.4 \text{ }\mu\text{m}$ . The contribution of the first  $n^+$  region to the photocurrent is found to be of great importance. Moreover, the photocurrent  $J_1$  exhibits a high value in the wavelength range from  $0.6 \text{ }\mu\text{m}$  to  $2.1 \text{ }\mu\text{m}$  due to the high excess carriers generated under light illumination. The photocurrent  $J_i$  (for  $i = 2$  and  $3$  regions) increases in the wavelength from  $2 \text{ }\mu\text{m}$  to  $2.4 \text{ }\mu\text{m}$  when the depletion photocurrent contribution is neglected for all wavelengths.

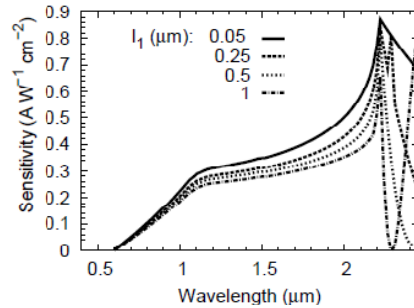


Fig. 3 Responsivity per unit surface of the  $n^+nn^+$   $\text{In}_{0.53}\text{Ga}_{0.47}\text{As}$  diode for different length value  $l_1$  with the structure is the same as that of Fig. 2.

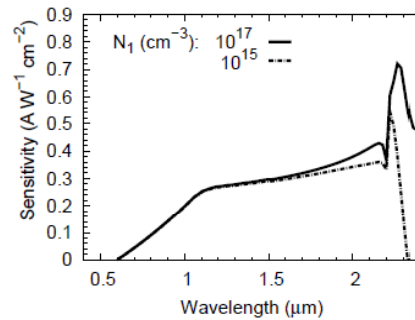


Fig. 4 Responsivity per unit surface of an  $\text{In}_{0.53}\text{Ga}_{0.47}\text{As}$   $n^+nn^+$  diode for different free carrier concentration  $N_1$  with:  $N_1 = N_3$ ,  $N_2 = 10^{14} \text{ cm}^{-3}$ ,  $l_1 = l_3 = 0.5 \text{ }\mu\text{m}$  and  $l_2 = 0.25 \text{ }\mu\text{m}$ .

Fig. 3 presents the sensitivity of an  $\text{In}_{0.53}\text{Ga}_{0.47}\text{As}$   $n^+nn^+$  Photodetector by using the results of Fig. 2.

Fig. 3 shows that when the device length decreases (when  $l_1$  decreases) the photosensitivity increases. In addition, the sensitivity of the  $n^+nn^+$  diode with  $l_1 = 0.05 \text{ }\mu\text{m}$  is more and about double than the sensitivity of the device with  $l_1 = 1 \text{ }\mu\text{m}$  length. This means that the  $n^+nn^+$  nanostructure can give better sensitivity at higher wavelength range.

The sensitivity of  $n^+nn^+$  photodetector in Fig. 4 is calculated for different free carrier concentrations.

We remark that the sensitivity presents an important value corresponding to a doping of  $10^{17} \text{ cm}^{-3}$  due to the increase of excess carriers photo-generated in the structure. Therefore, the low doping leads to limit the photocurrent generated inside the device.

Fig. 5 represents the static spectra of fluctuations of the drift-current flowing through the  $n^+nn^+$  diode calculated in accordance with (10) for different fixed values of the  $n^+$  region length (11). The analytical approach of  $n^+nn^+$  spectral current noise is developed in [10].

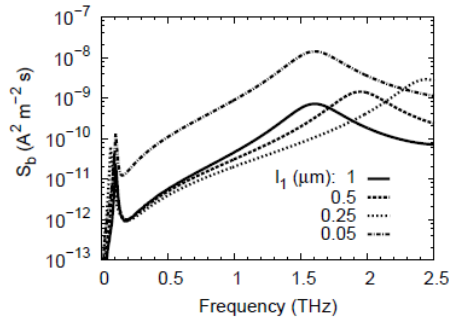


Fig. 5 Spectral density of current fluctuations per unit surface in a  $\text{In}_{0.53}\text{Ga}_{0.47}\text{As}$   $n^+nn^+$  diode for different  $l_1$  value with:  $l_1 = l_3$ ,  $l_2 = 0.25 \mu\text{m}$ ,  $N_{1,3} = 10^{17} \text{ cm}^{-3}$ ,  $N_2 = 10^{14} \text{ cm}^{-3}$ ,  $\nu_i = 0.1\omega_i$ .

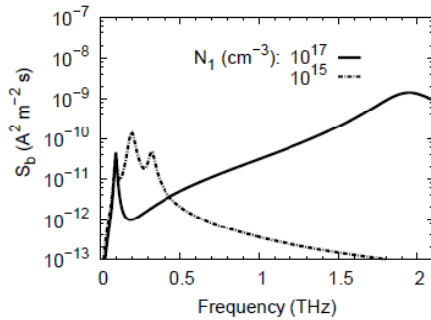


Fig. 6 Spectral current density per unit surface in an  $\text{In}_{0.53}\text{Ga}_{0.47}\text{As}$   $n^+nn^+$  diode for different free carrier concentration  $N_1$  with the structure is the same as that of Fig. 5.

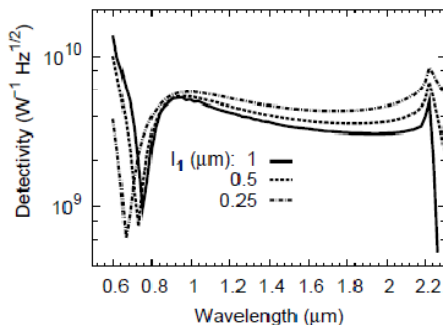


Fig. 7 Detection parameter of an  $n^+nn^+$  diode

As follows from Fig. 5, one can separate two areas in the  $S_b(\omega)$  spectrum, the low-frequency plateau where the thermal noise is considered and the high frequency where the noise is related to the free carrier fluctuations. We remark that the frequency position of the resonance peak increases when the length of an  $n^+$  region decreases (total length decreases) according to (6) and (7). Moreover, the free carriers fluctuations in (6) appear with the decreasing of  $l_i$  (appears in a nanostructure) when the thermal noise is dominant with increasing of the device length. Therefore, the contribution of the thermal noise in (7) may be neglected in nanostructure compared to the high geometrical structure.

In Fig. 6, we remark that the current noise spectrum exhibits a significant variation with free carrier concentrations. Moreover, the resonance peak appears near the frequency 2 THz for the doping value  $10^{17} \text{ cm}^{-3}$ . The spectral current noise increases with the increasing of the doping according to the plasma frequency  $\omega_i = \sqrt{(e^2/\epsilon\epsilon_0 m)N_i}$ .

We report in Fig. 7 the detection parameter for different  $l_1$  length values obtained by (11).

We remark that the detection parameter is proportional to  $10^{10} \text{ W}^{-1}\text{Hz}^{1/2}$  for the wavelengths range 0.6-2.3  $\mu\text{m}$ . Moreover, we observe the appearance of two high peaks of detection parameter near 1  $\mu\text{m}$  and 2.3  $\mu\text{m}$  corresponding to the presence of sensitivity peaks (see Fig. 3). The two peaks of sensitivity (Fig. 3) due to the important absorption of the  $n^+$  and  $nn^+$  homojunctions.

This means that the detection parameter of an  $n^+nn^+$  diode takes a constant value for the majority absorption wavelength range. On the other hand, the detection parameter decreases in low wavelength  $\lambda \leq 0.8 \mu\text{m}$  due to the increasing of the spectral current density value ( $S_b$ ) according to (11). In addition, we notice that by going from  $l_1 = 1 \mu\text{m}$  to  $l_2 = 0.25 \mu\text{m}$  the detection parameter of an  $n^+nn^+$  diode increase.

## V. CONCLUSION

We have presented an analytical model to calculate the sensitivity, the spectral density of the current fluctuations and the detection parameter in an  $\text{In}_{0.53}\text{Ga}_{0.47}\text{As}$   $n^+nn^+$  diode. The model allows us to describe precisely the high-wavelength part from 0.4  $\mu\text{m}$  to 2.3  $\mu\text{m}$  of the detection parameter. In particular, the dependence of the detection parameter to the device parameters, such as the free carrier concentration and structure length, is discussed at an absorption wavelength range of the  $\text{In}_{0.53}\text{Ga}_{0.47}\text{As}$  material.

The discussion of detection parameter results confirms that the homojunction  $n^+nn^+$  nanodiode has shown a good capability for infrared wavelength photo-detection. Moreover, the responsivity and spectrum current noise results can be useful for optimizing the device parameters for the infrared spectrum detection between 0.4-2.3  $\mu\text{m}$ .

The evaluation of the current noise in an  $\text{In}_{0.53}\text{Ga}_{0.47}\text{As}$   $n^+nn^+$  structure can determine the appearance of the intrinsic resonance noise in low and high frequency and their dependence on the total length and doping of the diode. The spectral current density results improves that the  $\text{In}_{0.53}\text{Ga}_{0.47}\text{As}$

$n^+nn^+$  structure is useful in high frequency operation as an infrared detector.

#### ACKNOWLEDGMENT

This work is partly supported by the Algerian ministry of higher education and research through contract N. D03820100006 and by TeraLab-Montpellier.

#### REFERENCES

- [1] D. D. Coon, R. P. Devaty, A. G. U. Perera and R. E. Sherriff, *Journal of Applied Physics Letter*, vol. 55, 1989, 1738.
- [2] A. G. U. Perera, R. E. Sherriff, M. H. Francombe, R. P. Devaty, *Journal of Applied Physics Letter*, vol. 60, 1992, 552.
- [3] C. Balocco and al., *Journal of Applied Physics Letter*, 98, 2011, pp. 223501.
- [4] Nibir K. Dhar, Ravi Dat and Ashok K. Sood, *Optoelectronics-Advanced Materials and Devices*, 2013, DOI: (10.5772/51665).
- [5] F. Z. Mahi and L. Varani, *IEEE proceedings 22<sup>nd</sup> Int.Conf. On Noise and Fluctuations*, 24-28 June Montpellier, 2013, DOI: (10.1109/ICNF.2013.6578930).
- [6] F. Z. Mahi, A. Helmaoui, L. Varani, C. Palermo, P. Shiktorov, E. Starikov and V. Gruzhinskis, *Fluctuations and Noise Letter*, 2011, vol. 121.
- [7] B. K. Mishra, L. Jolly, S. C. Patil, "In<sub>1-x</sub>Ga<sub>x</sub>As next generation material for photodetectors", *Journal of Selected Areas in Microelectronics (JSAM)*, April Edition, 2011.
- [8] F. Z. Mahi, A. Helmaoui, L. Varani, P. Shiktorov, E. Starikov and V. Gruzhinskis, *Physica B*, vol. 403, 2008, 3765768.
- [9] L. Reggiani, P. Golinelli, E. Faucher, L. Varani, T. Gonzalez and D. Pardo, *Proc. 13th International Conference on Noise in physical systems and 1/f fluctuations*, Eds. V. Bareikis and R. Katilius. World Scientific Singapore, 1995, 163.
- [10] F. Z. Mahi and L. Varani, *Results in Physics, Published by Elsevier* 3, 2013, 209.